Temperature regulation of concentrating photovoltaic window using Argon gas and Polymer Dispersed Liquid Crystal Films

Maria Khalid[1], Katie Shanks, Aritra Ghosh, Asif Tahir, Senthilarasu Sundaram, Tapas Kumar Mallick[2]

Environment and Sustainability Institute, University of Exeter Penryn Campus, Penryn, TR10 9FE, UK

Abstract: Low concentrating photovoltaic (LCPV) system has been studied extensively, which showed excellent potential for the building integration application. However, such a system suffers from higher operating temperatures due to the concentrated light exposed into the solar cell. In this work, two different methods have been used to regulate the operating temperature of the solar cell without the interference of any other external mechanism. Two concepts were used to study the operating temperature of the solar cells are: i) use of Argon gas within the concentrator element, ii) incorporation of polymer-dispersed liquid crystal films (PDLC) on top of the module. In both cases, the power was improved by 37 mW to 47 mW when temperature was reduced by 10°C and 4°C for the Argon gas-filled module and PDLC integrated module, respectively. In addition, the temperature effect of the PDLC integrated module showed a unique nature of reduction of the short circuit current due to the orientation of the liquid crystal particle, which increased at a higher temperature. The current study, therefore, shows the greater potential of improving the operating efficiency and reduction of solar cell temperature, without the need for additional pumping power such as needed for photovoltaic thermal application.

Keywords: Square elliptical hyperboloid concentrator; BIPV, Electrical and thermal characterisation, Polymer dispersed liquid crystal.

1. Introduction

In recent times, the low concentrating photovoltaic (LCPV) by using optical concentrators such as lenses mirror to focus incident radiation on the smaller area is an appealing application in photovoltaic industry for low cost and higher yield solar power generation. LCPVs trim down the cost of the PV system by reducing the cell area and replacing expensive semiconductor material by inexpensive semiconducting material [1–4]. LCPV does not require expensive tracking system, supply more power for a limited area which reduces the necessity of large areas fragile silicon PV, and simpler system for building integration [5] [6][7]. In general concentration ratio of LCPV for building integration remain <10 [8].

Non-imaging compound parabolic concentrator (CPC) is one of the most studied LCPV system, suitable for building integration [9], due to its higher acceptance angle [10] [11]. CPC includes reflective or refractive mirror [6] or dielectric [12] type; symmetric [13] or asymmetric [9]; 2-dimesional [14] or 3-dimensional [15] type optics.

Most studied CPC geometry for building integration is 2D symmetric and asymmetric type which accept all the incident rays within the acceptance angle however it rejects all other incident radiation which is outside the acceptance angle [16,17]. The lumped electrical model was designed with 2D asymmetric CPC (trough) to measure their IV curves in an indoor laboratory. This model was integrated successfully to examine the coupled optical-thermal-electrical performance of CPC [14]. In northern latitude location, dielectric asymmetric compounds parabolic type showed un-stability at higher acceptance angle. Further work was needed to investigate the effect of change in the solar spectrum over time by

[1] Corresponding Author: Email: mk636@exeter.ac.uk;
[2] Email – t.k.mallick@exeter.ac.uk

considering the refractive index of the dielectric material and dispersive absorption coefficient followed by low-cost manufacturing process [9]. Limited concentration obtained from 2d geometry can be increased by using 3d CPC. However, 3d geometry offers circular exit and entry aperture which produce more losses and circular shapes PV cells are not popular. Thus, to enable the use of 3d CPC for rectangular or square shape crystalline silicon PV cells, crossed compound parabolic concentrator (CCPC) was developed which is 3d in nature and intersection of two 2d CPC crates this shape. A 3D crossed compound concentrator based on dielectric was used to analyse energy transformation and energy output of a low concentrated PV system [12]. Another 3D CCPC based PV module was fabricated to determine optical and electrical performance for building façade integration [11]. To improve further the concentration ratio, there are however other LCPV optic designs which require further investigation such as the Square-Elliptical-Hyperbolae (SEH) optic by Sellami et. al. [18] which is shown in Fig. 1. This SEH has elliptic entry to the square exit. This system had a concentration ratio of 6x, the optical efficiency of 55% and an acceptance angle of 50°, however, the concentration of incident light was non-uniform at the solar cell. SEH based spaced type LCPV BIPV window can be the next generation system which will have triple advantages into the building application: i) maintaining daylighting within the building envelope, ii) reduce thermal load of the building and iii) generate electricity within the building envelope. Thus 2D, 3D CPC are not compact, and they need to truncate the upper reflector section to maximize the efficiency of the BIPV. This new design is compact enough and feasible for BIPV application and can be accurately integrated into transparent façade, windows or roofs.

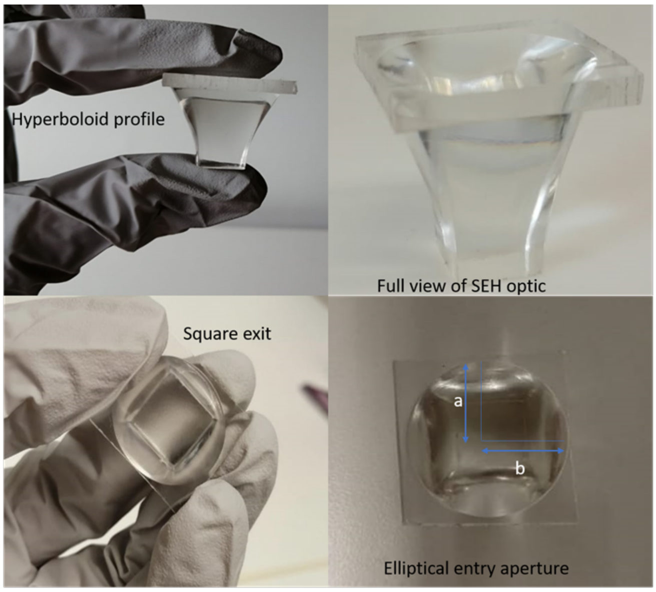

Fig. 1: Dimension description of SEH based LCPV system used in this experiment

An important parameter that can negatively affect the performance of the PV cell is the temperature sensitivity of the solar cell. PV cells experience high thermal energy due to the absorption of incident solar radiation that is not converted into electricity. Several researchers have investigated the comparison between theoretical temperature and different parameters that come from solar cell output [19][20]. Bett et al. calculated theoretical values' illustrating that temperature coefficient is dependent on the dominant recombination process. Another group from NREL measured experimentally the metastable changes due to light exposure results as the temperature dependence of the fill factor of CIGS that modified thin-film cells [21]. It is well studied the efficiency of the solar cell, overall power output and open-circuit voltage decreases due to the increase in solar cell temperature [22]. Variation in external quantum efficiency (EQE) also seen due to temperature variation in different regions of spectra. The influence of temperature of PV cell on different mechanisms fill factor (FF), open-circuit voltage (V_{oc}), short circuit current (J_{sc}) are well known. The fill factor temperature sensitivity can be possibly due to technical issue such as contact resistance [23]. Electrical performance of a typical PV module is 18-24% of the incident solar radiation, dependent on climate condition and type of solar cell used in the module. The rest of the incident radiation is converted into heat that can be primarily cause of increment of temperature and reduce the efficiency of the PV module [24].

Enhanced temperatures of crystalline silicon based solar cell under solar radiation is an important issue [25,26]. This becomes worse when the light is concentrated; specifically for the silicon solar cell and light concentrated on the solar cell surface, a significant rise in temperature is evident [27]. Thermal regulation of crystalline PV cells is thus essential for concentrating system. Thermal regulation using active air and water cooling and passive air cooling is possible and has been demonstrated as an effective and economical way. The proper length of the fins to pint out the harassment of the power of the PV system was inquired during the passive cooling by phase change material [28]. However, water- and air-cooling techniques need the additional cost of pump or fan to maintain the output of the system. In the case of water, evaporation is another obvious drawback to giving lower efficiency [29]. The incorporation of phase change materials into PV systems with concentrator photovoltaics can enhance the performance of the system in warmer weather of UAE [30]. Phase change materials absorb thermal energy as latent heat and can be used to maintain the temperature of the PV system at suitable phase transition temperature [31][32].

Previously, phase change material (PCM) type temperature regulation has been demonstrated by Sharma et al.[33] for low concentrator system. BIPV façade systems for temperature regulation with the induction of complicated airflow and convective heat transfer through natural way has been reported [34].

Simple method without compromising electrical efficiency of PV panels is natural cooling using free convection to remove heat from the back of the PV modules. A heat sink for CPV using normal grade aluminium on the back of the PV module to remove heat by thermal conduction has been examined. With a concentration of 500 suns, this system was capable to reduce cell temperature by up to 10°C [35]. For passive cooling of PV cells heat pipes were used; 38°C temperature was reduced [36]. Hydronic cooling technique was induced with the PV system to minimize the operating temperature; consequently, 23°C reduction was evident with an increase of cell efficiency of 3.26% [37].

Spaced type concentrating BIPV window systems are mostly double glazed which further needs modification to enable it for heating load dominated location. Replacing the air between two glass panes with inert gas [38][39][40] or vacuum [41,42][43] can offer higher thermal insulation. Spaced type concentrating BIPV windows also offer static transparency which can be modulated by using smart switchable materials. Current switchable materials are electrically, thermally or optically activated, where electrically activated types such as electrochromic (EC), polymer dispersed liquid crystal (PDLC), and suspended particle device (SPD) respectively, are favourable due to their user control behaviour [44]. PDLC type smart materials become transparent in the presence of AC power supply and translucent while no power is applied[45–47] . The translucent state provides a lower transmission but provides full privacy from viewing which is suitable for glare control. PDLC glazing as a suitable candidate for building façade application has been the subject of many researchers [48]. PDLC glazing performance for overcast cloudy day was also examined and was acceptable to control glare [48]. However, no such work reported for the use of PDLC for CPV applications. The reliability and endurance of concentrated BIPV technology with PDLC requires more research and use of alternative materials for novel applications.

The integration of argon gas as insulating material within the panes of double-glazed window is another significant process to enhance the thermal insulating performance. Double glazed windows with argon gas filling approach has lion's share in window technology and can represent an effective energy saving solution. U-value assessment of commercially available argon double-glazed window was examined numerically, experimentally, and theoretically. The experimental results were quite ample from environmental chamber tests showing good accordance with theoretical datasheet [49]. Another work was reported to present comparison of thermal performance of coated double- glazing and non-coated double-glazing with same argon gas filling ratio [50]. The U-value of non-coated double-glazing reduced about 3.7% and 13% for coated double-glazing. Moreover, the relative energy with low emissivity coating of 0.13 was saved about 51% making this system suitable to meet requirement of building energy efficiency.

Although, this approach has downside of drastically reduction in amount of solar radiation to pass through the glass due to insulating material. However, this condition has advantageous and disadvantageous behaviour at different latitudes such as it gives favourable output at medium latitude such as central Europe and unfavourable output at higher latitude areas e.g. Scandinavian countries.

In this work, an LCPV window prototype containing the SEH CPV module was modified using Argon gas within the double-glazed window cavity to improve insulation characteristics and PDLC film covers to control the daylighting and operating temperature. This developed system has been used for testing of PV module performance for different parameters such as efficiency, FF, power output and operating temperature of the system. Presence of argon gas and polymer dispersed liquid crystal (PDLC) film's thermal behaviour of PV cells in a concentrating BIPV window has been investigated under indoor condition.

2. Materials and methods:

The prototype LCPV optic utilised in this work is made up of three different types of geometries: an elliptical entry aperture; a hyperbolic profile section, and a square exit aperture, developed and experimented previously [18]. The elliptical entry aperture was designed to capture the maximum of natural light by maximizing acceptance angle. When arranged in an array, the space between the elliptical entry apertures allows semi-transparent windows to be produced. The square exit aperture of the SEH aims to reduce the cost of the system by reducing the solar cell material required. This shape was more convenient as it is similar to the shape of the solar cell to give reliable efficiency. The third geometry was a hyperboloid shape that was combined with both above-mentioned geometries to design a novel geometry. The SEH optic has 6× geometric concentration. The top elliptical shape has total inlet aperture area of 66mm2 with two semi axis, a=13.06mm and b=9.75mm. The area of the base is 10mm equal to area of silicon cell. Whereas, the length of the optic element is 25mm. The equation used to design the geometry of the optic are shown elsewhere [18]. The total dimension of the module is 224 mm by 160 mm.

The two set-ups used in this work are:

- System 1: Argon filled low heat loss concentrating BIPV window module as shown in Fig. 2. During this process, the Argon (Ar) gas was filled within the air gap of the module (as shown in Fig. 2, between the optical profiles) for 30 minutes. The silica-based sealant was used to keep the gaseous medium within the system. This system was studied extensively with and without the Ar gas for an identical period.

- System 2: PDLC based films were used on top of the glass cover shown in Fig. 2. The experiments were carried out for both the ON and OFF modes of the PDLC. The thermophysical properties of the system is given in table 1 and the table 2 shows the solar cell parameters. The solar cells were manufactured by Solar Capture limited.

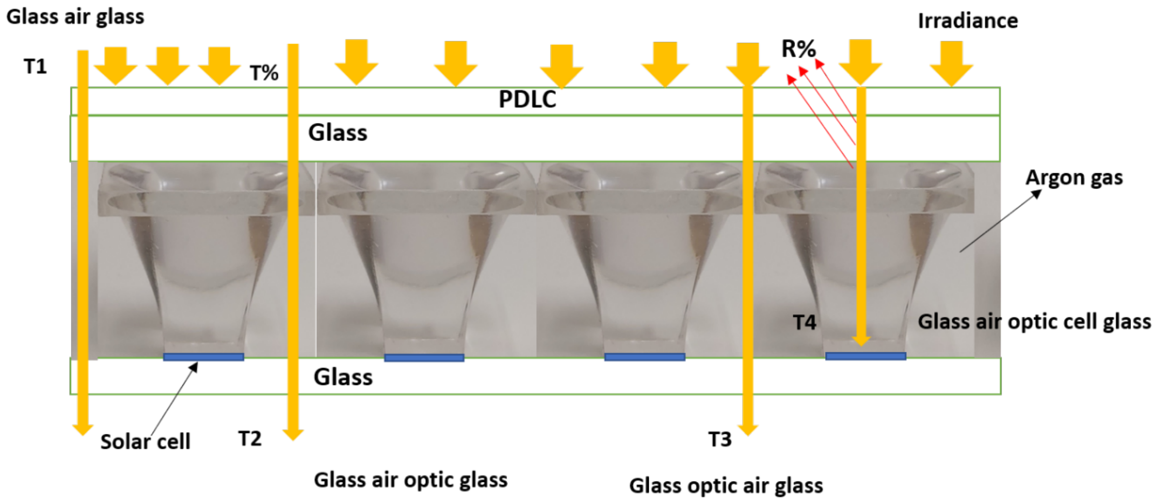

Fig. 2: Diagram shows the light incident, reflected and transmitted of the integrated module through its different parts of the system.

Material	Thermal Conductivity (W/mK)	Refractive Index
Glass (Crown: CDGM –K)	0.96-1.05	1.523
Argon gas	0.018	1.002
Crystal Clear (Urethane Resin)	~0.2	1.499
Air	~0.024	1.0003
System Dimension	224mm × 160mm	
Number of Solar Cell	16	

Table 1: Thermophysical properties of the SEH system

Dimension	10 mm x 10 mm
Solar Cell type	LGBC Silicon cells
Short circuit current	455 mA
Open circuit voltage	0.55V
Fill factor	79%
Efficiency	17%

Table 2: Solar cell parameters

In this work, the following experiments were carried out:

- Using Parkin-Elmer 1050 spectrophotometer, the optical properties of the samples were measured for the System 1 with and without Argon. In addition, the optical properties of the System 2 were measured while the PDLC films were in the ON and OFF mode. During these experiments, transmission and reflectance were measured for a wide range of wavelength at the different section of the module as shown in Fig. 2.
- Both configurations of the LCPV module (System 1 and System 2) were extensively tested to measure its thermal and electrical properties under the controlled solar simulator. The experimental setup for the thermo-electrical testing of the system is shown in Fig. 3. It used an $A^+A^+A^+$ WACOM sun simulator, IV-Tracer, data acquisition system and controller. The temperatures were measured using K-type thermocouples.

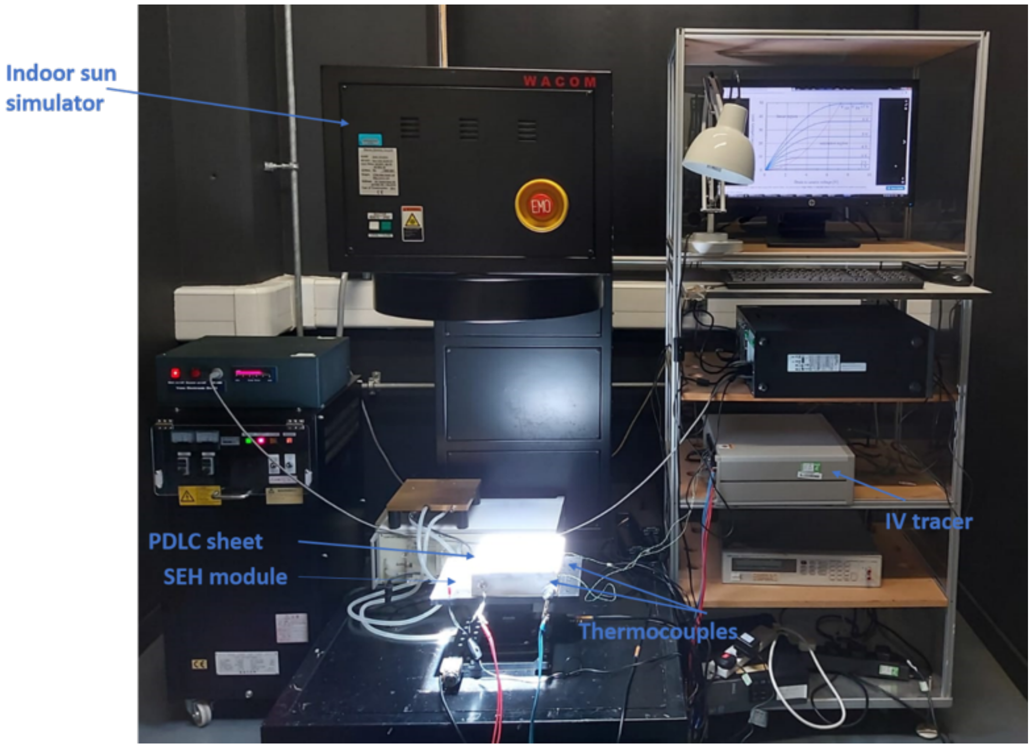

Fig. 3: Schematic diagram of Square-Elliptical Hyperbola LCPV optic experimental setup consisting of with all connections of the system

3. Results and Discussions

3.1. Optical Characterisation

The transmittance spectra of the SEH LCPV system at different positions were measured for a range of wavelengths from ultra-violet to near-infrared (UV/VIS/NIR) ranging spectrometer from 250 nm-2000nm for Ar gas-filled module and without filling of Ar gas. For PDLC, both opaque and transparent mode transmittance spectra were measured for 250nm-2500nm range. To fully understand the optical losses within the module, measurements were taken at three different positions. The transmission spectra for the SEH LCPV system without the Argon (Ar) gas and with Ar gas are shown in Fig. 4.

In Fig. 4 (a), the average transmission of the single optic was 85% between 300 nm to 2000 nm which is expected not only due to absorption but due to lighter scattering. As it could not measure straight through the optic due to cell and TIR properties without cell. For the first position (T1 in Fig. 2) gave the transmittance through the two cover glasses and inner air medium glass-air-glass(GAG) which had the maximum transmittance of ~99% and average transmittance of 64% between 300 nm and 2000 nm as shown Fig. 4.

The glass air optic glass (GAOG) has an average transmittance of 65%, covering the wavelength range from 300nm to 1100nm. The lowest transmittance is 50% given by glass optic air glass (GOAG) within range of 370nm to 2000nm that indicates of how much light is being scattered not to the cell but instead into the room different font. As it can be seen in Fig. 4(a), for most of the visible range, the transmittance spectra remain almost constant for all four different samples. However, the transmission goes down in a significant manner in the NIR regions, which improves provides better performance of the crystalline silicon solar cell. Due to the higher transmission of the single optics (SO), the electrical efficiency of the solar cells is likely higher than into the other regions of the spectrum.

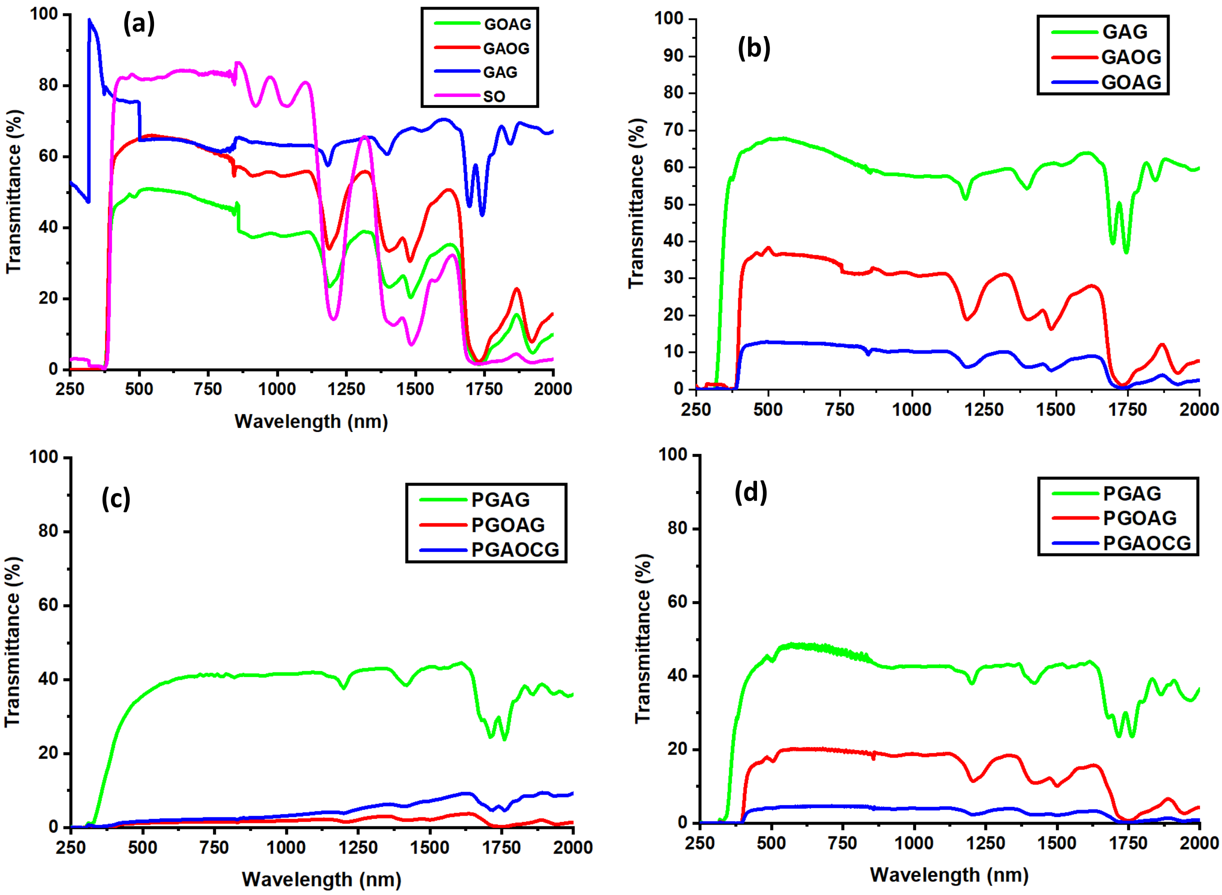

Fig. 4: Transmittance spectra measured through SEH LCPV system using a spectrometer (a) without Argon gas, (b) with Argon filled, (c) with PDLC film on top of the modules while OFF state and (d) with PDLC film on top of the module while ON state.

The transmittance spectrum of the SEH module filled with argon gas is measured as shown in Fig. 4(b). The transmittance data for argon-filled system showed variation with constant applied power. Within ultraviolet an increase can be seen while in the visible region from 380nm to 700nm it showed nearly constant behaviour. Therefore, near-infrared region variation in wavelengths shown has the highest transmittance of 68% for glass air glass and 38% for glass air optic glass. While the lowest transmittance is for glass optic air glass that showed 13% light is scattered for light incidence between the optics entry apertures and so suggests unclear viewing for people looking out of the window, which may be important depending on the application. But this is a prototype so an optimised manufacturing method may smooth out the intersections of the optical material and hence gives clearer more aesthetic viewing between optics different fonts.

The transmittance of the system by placing polymer dispersed liquid crystal film is examined for both on and off state and showed a clear trend of variation. For PDLC off state, highest transmittance is 45% for PDLC glass air glass (PGAG), 9% for PDLC glass air optic cell glass (PGAOCG) and PDLC glass optic air glass (PGOAG) has the lowest transmittance of 3% as shown in Fig. 4(c). While PDLC on state Fig. 4(d) showed maximum transmission of 49% for PDLC glass air glass, 20% and 4% for PDLC glass optic air glass and PDLC glass air optic glass respectively. Therefore, different transmission spectra confirm that the effect of Argon gas and PDLC film on the LCPV system provide adequate differences in their optical properties for a wide range of wavelength of the solar spectrum.

3.2. Temperature dependencies and effect on power output:

The thermal performance of the system was investigated as per the experimental procedure described in Fig. 3. The samples were exposed to solar radiation over one hour to stabilise the temperatures until the equilibrium is reached. During this period measurements were taken in intervals of 10 minutes. Fig. 5 shows the variation in temperature of the solar cell (the temperature sensor was placed as shown in Fig. 3) while the solar radiation intensity was constant to 1000 W/m^2. The temperature variations were measured for all four scenarios: with Argon gas, without Argon (Ar) gas, with PDLC in OFF state and with PDLC in the ON state. The solar cell temperature for the gas air-filled system (no Ar) varied from 26°C to 52°C after 57 min of exposure, while the solar cell temperature reached only to 45 degrees in the presence of Argon gas. During the first 10 min of exposure temperature of the solar cell without Argon gas increased sharply from 26°C to 34°C, while the rate of increase during the same period for the LCPV system with Argon gas inside slowed down the temperature increase. This is possible due to the inert nature of gas, which effectively reduces the heat transfer coefficient, amounting lower temperature of the glass. The start temperature of the solar cells was same when the experiment started for the system with PDLC films as “OFF” state, it achieved higher temperature as compared to the LCPV system with PDLC “ON” state. The rate of increase of temperature for the solar cell while the PDLC was ON state was lower than that of during the Argon filled gas system. Due to the activation of the PDLC, the temperatures were higher when the PDLC film was ON state, clearly providing the better thermal performance of the solar cell as compared to the OFF state. Although the rate of temperature increase of the PDLC film was lower than that of the other systems at the beginning of the experiment, the peak temperatures were same for both the Argon filled system and the PDLC switched OFF system.

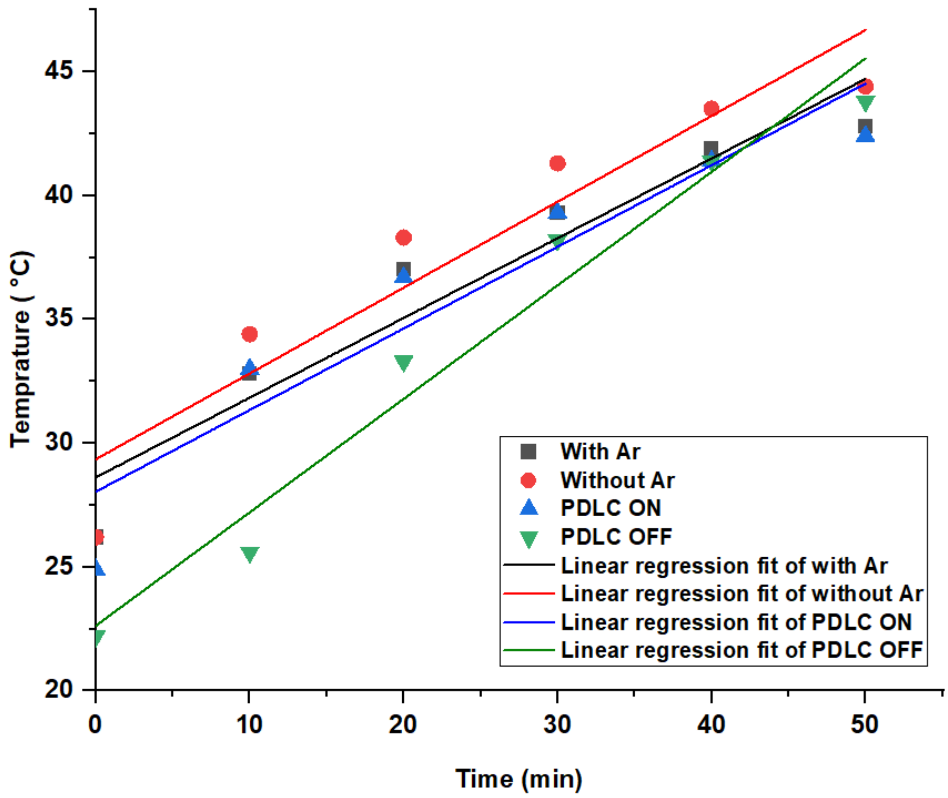

Fig. 5: The variation of the solar cell temperatures during light exposure for the LCPV system for with/without Argon gas and with PDLC opaque and transparent mode

3.3. Electrical performance of the LCPV system with and without Argon gas:

The electrical performance of the SEH-LCPV system was carried out to measure the I-V curves, FF and the solar to electrical efficiency of the modules at different temperatures. The I-V characteristics of the solar cell of the module with cell temperature before filling Ar gas and after filling Ar gas at constant light intensity are presented. Measurements were taken at the same time intervals for Ar gas-filled and without Argon gas. It is clearly visible in Fig. 6 that the open-circuit voltage, and hence cell efficiency decreases with increasing temperature as expected in the standard solar cell properties. As, short circuit current is most dependent on the radiance of light and open circuit voltage is dominated by cell temperature, as increasing cell temperature, reduces the CPV system's overall power output, efficiency and open-circuit voltage. The most sensitive parameter of the solar cell is open circuit voltage that is dependent on temperature. Similar to the standard flat plate Silicon based solar module the temperature behaviour remains same i.e. the temperature coefficient of open-circuit voltage is negative as well as positive for the short circuit current.

Fig. 6b depicts the variation of IV characteristics for different operating solar cell temperature of the SEH LCPV system for Ar filled. Measurements are taken at same time interval as for without Argon gas. At beginning, at uniform light intensity of 1000 W/m^2 value of short circuit current is 150mA and open circuit voltage is 830mV and further plummets. For the first measurement, the cell temperature is 31°C that moderately goes on increasing to 35°C, 38°C, 39°C, 41°C 42°C and 44°C. A maximum power improved by 37mW was noticed for the system filled with the Argon gas. It is obvious from Fig. 6b there is a significant increase in FF at the same certain time intervals. As argon gas is denser than air and has lower thermal conductivity as well so it can improve the U-value of Argon glazing. Without argon gas, the temperature of the solar cell goes up due to higher thermal resistance as the incident light heats the glass panes but they do not transfer their heat so much to the cells and optics because Ar gas is denser than air.

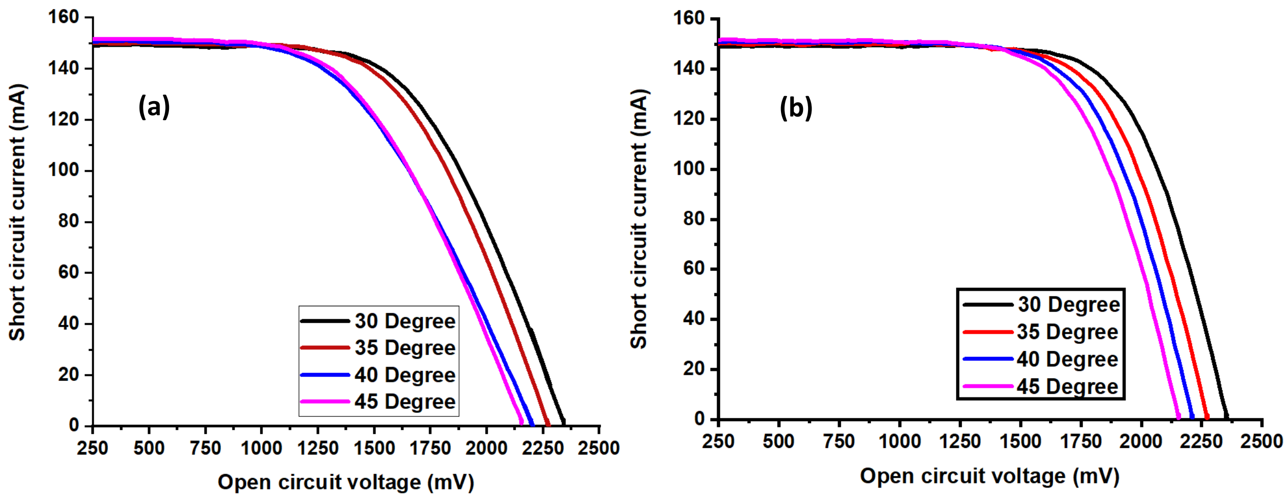

Fig. 6: Current-voltage curves for the different temperature of the SEH module (a) without Argon gas and (b) with Argon gas.

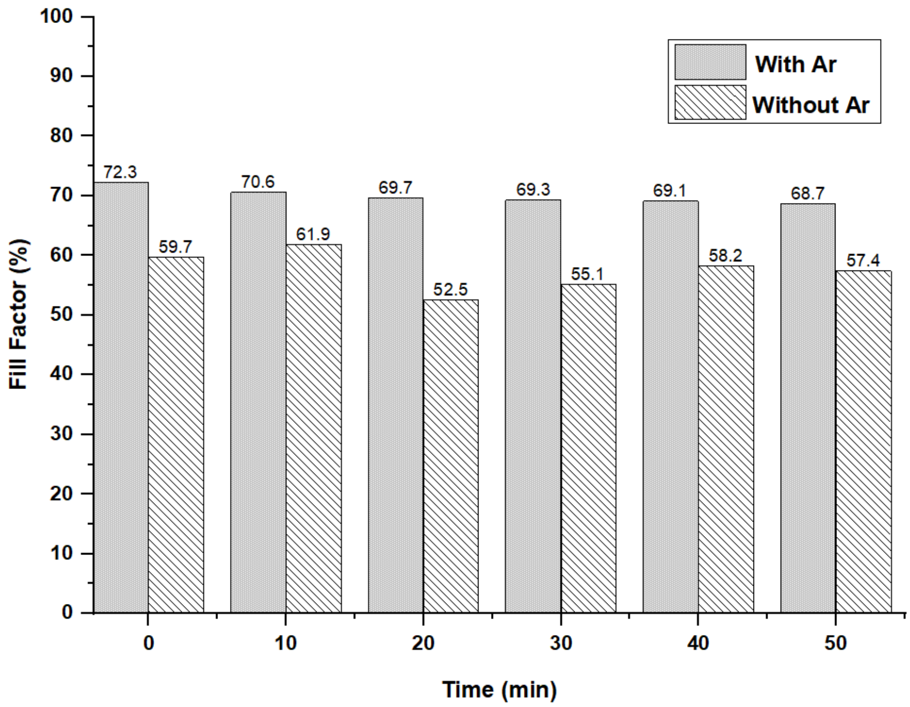

Fig. 7: Variation of fill factor with the time of exposure for the CPV window with and without Argon gas

The FF exhibits the maximum power output that can be extracted from short circuit current to open-circuit voltage, also the minimal obtained cost of photogenerated charges from the cell into the circuit. The output of FF also depends on contact resistance that can be caused by technological issues such as carrier transport. The FF of the PV module can be calculated using following equation:

$$FF = \frac{P_{\max}}{V_{oc} I_{oc}} \qquad (1)$$

In the current study, at different intervals of time, FF was measured for both conditions of PV system with Argon gas and without Argon gas. The Fig. 7 shows the variation of the FF with time of exposure for the CPV window when the system was filled with the Argon gas and without it. The fill factors were higher for the case of the CPV system filled with Argon as compared to the when Argon gas wasn't filled within the system. The maximum FF of 72.3% occurred for the system while Argon gas was filled whereas the maximum FF of 61.9% achieved when no Argon gas was present within the CPV system. While the FF went to its minimum value of 52.5% after 20 minute exposure of the module when CPV system wasn't filled with the Argon Gas. This is clearly due to the temperature rise as seen in Figure 5. While the FF remained almost same for 30, 40 and 50min of exposure for the CPV system when Argon gas was filled in, the fluctuation of FF occurred for the system without Argon gas during these times increasing from 55.1% to 58.2% and finally reduced to 57.4%. This is due to the internal resistivity changes during the longer exposure of the light onto the solar cell when the CPV system wasn't filled with the Argon. In addition as shown in the Fig. 5, the temperature was higher for the case of the CPV module in the absence of the Argon gas within the device.

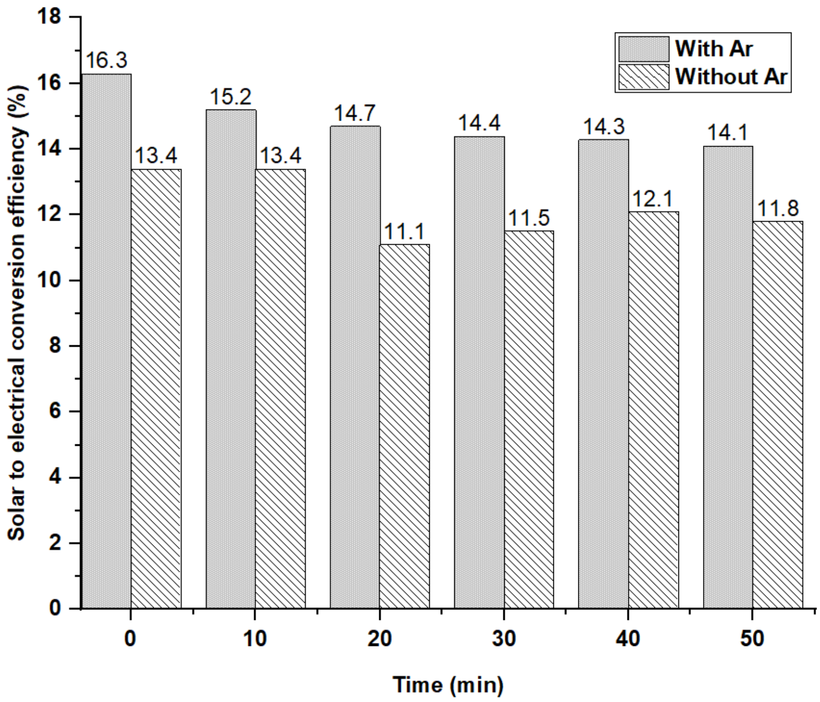

Fig. 8: Variation of efficiency with time of exposure for the CPV window with and without Argon gas

The solar to electrical efficiency of the PV system can be defined as ratio of electrical power output to the incident radiation as following:

$$\eta = \frac{P_{\max}}{GA} \quad (2)$$

The solar to the electrical conversion efficiency of the system was calculated for the same interval of time as for the FF for both conditions with and without Ar gas. Fig. 8 represents the variation of the efficiency with operating temperatures for the system when the device was filled with Ar gas and without any Argon gas into it. After exposure of constant radiation for 10 minutes system with Ar showed 16.3% efficiency. After a further 10 minutes of time interval efficiency decreased to 15.2% and remained about the same for the next three measurements. For the Argon filled system, typically the efficiency is higher than that of the system without the Argon gas. Measurements were taken at the same time interval as for without Ar gas. In the beginning, LCPV system showed 13.4% efficiency and after 10 minutes of exposure, efficiency remained the same for the next measurement as well. The drop in the efficiency can be due to optical mismatch which were agitated by increased temperature. For the next interval efficiency decreased to 11.1% and but again increased to 12.1% and kept almost remain same. The decrease in efficiencies for Silicon based solar cells has been reported earlier studies [51] , which is different than multi-junction solar cells [52]. This variation is very small, however this can be explained by the spectral losses of the optical device due to rise in temperature.

3.4. Electrical performance of the SEH CPV performance with PDLC film

The electrical performance measurements were carried out for the LCPV system with PDLC film for OFF and ON state. Fig. 9(b) shows I-V characteristics for different temperatures while the PDLC film was switched ON (transparent). While 9(a) shows the I-V characteristics for switched OFF (translucent) state. All measurements were done at similar time, indicated to provide similar boundary conditions for the measurement's scenarios. PDLC switched OFF had an average transmission of 45% which reduced the light transmission and offered lower Isc as shown in Fig. 9(b).

Almost 40% drop of Voc was observed when the temperatures were approximately 38°C and 42°C respectively. This is dropped primarily due to liquid crystal particle orientation when the temperature increased beyond a point called critical temperature. While the PDLC was OFF mode, the IV curves followed a similar pattern as of normal silicon solar cell's variation for different temperatures, however, the short circuit current increases more than expected with the temperatures between 30 and 45°C. overall, the short circuit current is reduced as compared to the PDLC ON state more as it implies that transmission reduced during the OFF state of the PDLC, as confirmed earlier from Fig. 4(c). In this case a maximum power output of 47mW was observed.

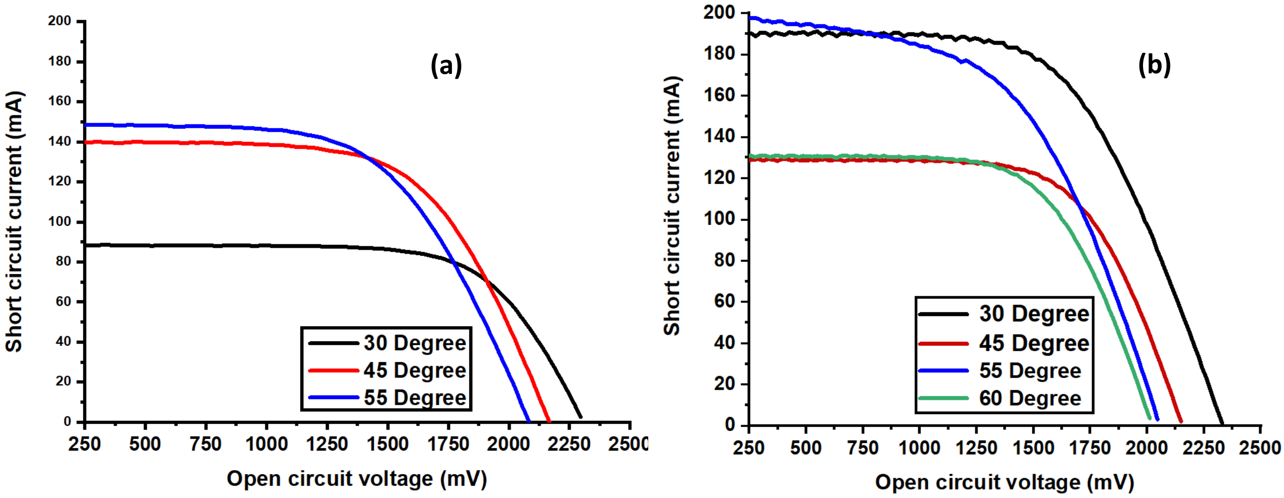

Fig. 9: Current and voltage characteristics of SEH module with the PDLC as (a) OFF state, and (b) ON state

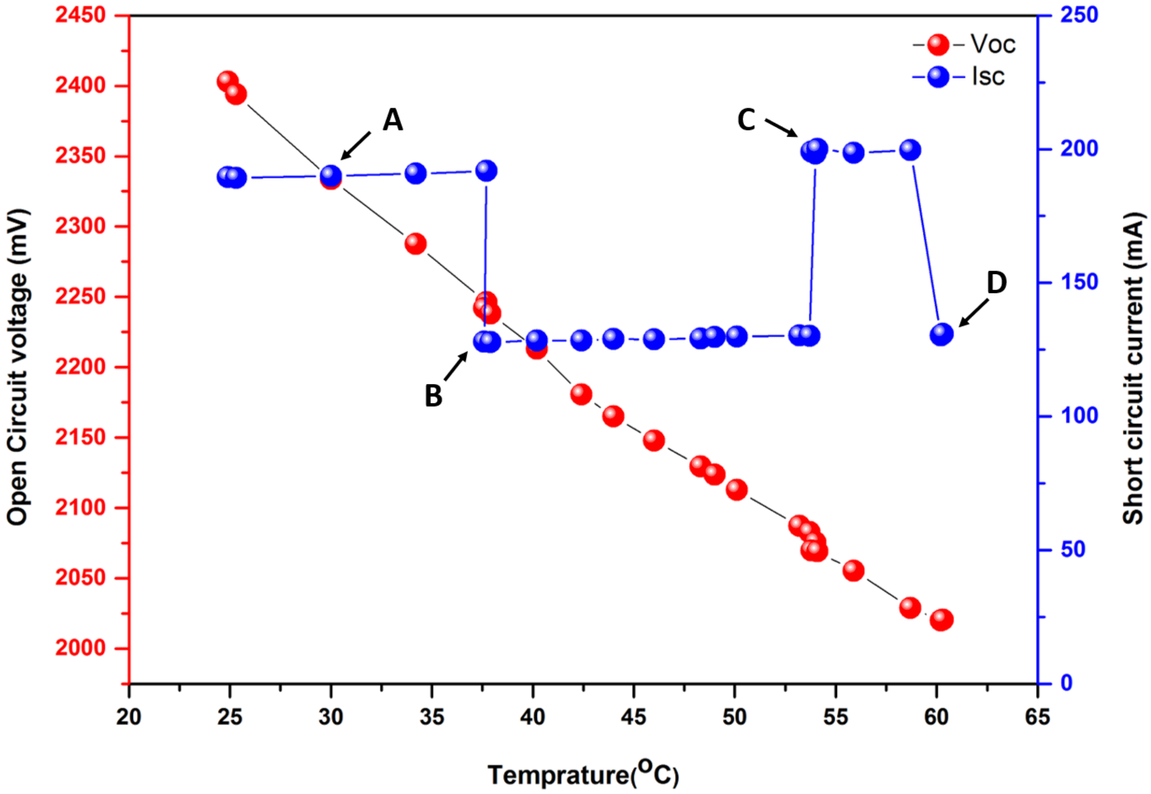

Fig. 10: Variation of the short circuit current and the open-circuit voltage of the integrated system when the PDLC was at ON state.

Fig. 10 depicts the variation in temperature with the short circuit current and the open-circuit voltage of the integrated device while PDLC is ON state. While the open-circuit voltage reduces linearly with the temperature an interesting phenomenon was observed for the short circuit current as seen in Fig. 10. With the exposure of constant radiation temperature of LCPV system arise to 30 degrees (at point A) but after a certain interval of time at about 37 degrees short circuit current (Isc) dropped from 200mA to 125mA (Point B) and remained constant till 54°C. Moreover, it increases at 55°C (Point C) to its maximum value of 200 mA and then, immediately reduced at 60°C (Point D) to 125mA and remained the same till the end of measurements. This unique phenomenon is explained in Fig. 11. Fig. 11 (a) represents off state of PDLC film when no power supplied to SEH system and PDLC showed translucent state. During this state, polymer liquid crystal particles dispersed into matrix orient randomly and do not allow incident light to pass through the film but few of them. Fig. 11(b) depicts on state PDLC that showed a transparent state. Through this state, liquid crystal particles are aligned and let light pass through the PDLC film. As a result, high transmittance achieved for the transparent state. Fig. 11 (c) shows Liquid crystal particles oriented as tilted position (this is the critical point i.e. point B or C in Fig 10) and the possible reason for it can be temperature goes up. This is called “critical point” for the PDLC to operate at an optimum temperature. During this state, PDLC let some of the incident solar rays pass through it but some of them scattered that cause higher temperature.

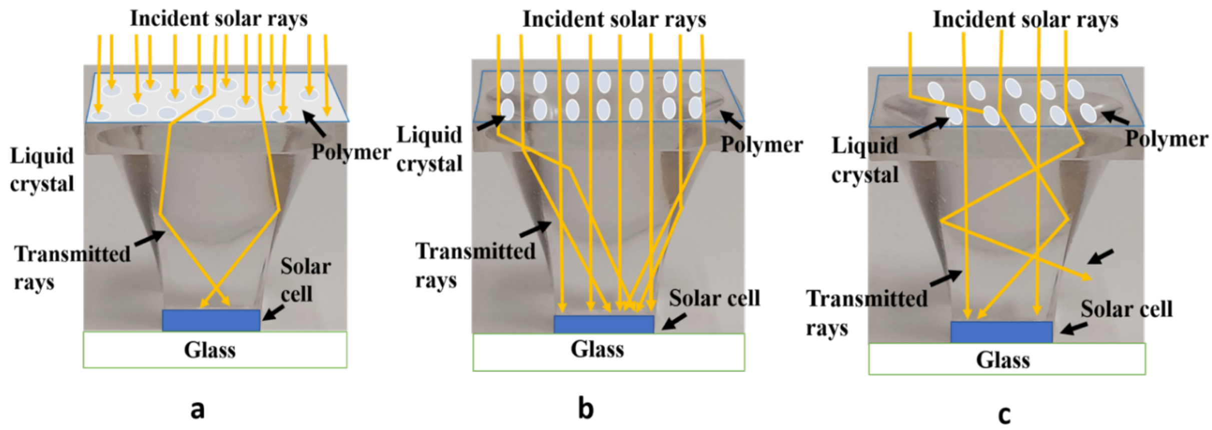

Fig. 11: Schematic diagram of double-glazing window with SEH LCPV system and the PDLC film on top of the module while its ON mode for different temperature variation: (a) normal operation of the integrated module when the operating temperature is within the range of 25-37°C, (b) when the integrated system operates in the range of 37-54°C and (c) when the integrated system operates in the range of 55-59°C.

Based on the IV measurements, the FF and the efficiency of the system were calculated during the time of the experiment. The FF of the module when the PDLC film was ON and OFF state is shown in Fig. 12. It was observed that the maximum electrical conversion efficiency of 9% and 6% achieved when the PDLC film was ON and OFF state. The variation of the efficiency of the module with PDLC ON and OFF state is shown in Fig. 13. It is interesting to observe that the minimum electrical conversion efficiency was observed for these two stages at a different time. It is obvious from Fig. 12 and 13 that the efficiency and the FF does not follow the same pattern for the LCPV module when the PDLC was ON state. In particular, when the PDLC is switched ON, the efficiency of the system increased from 4.4% to 6.3% and remains almost same. Also, this effect can be explained by the partial particle orientation as described in figure 11. This is due to the increase in temperature which affected the orientation of the particle sizes to allow more light passing through the optical device to generate more electrical power.

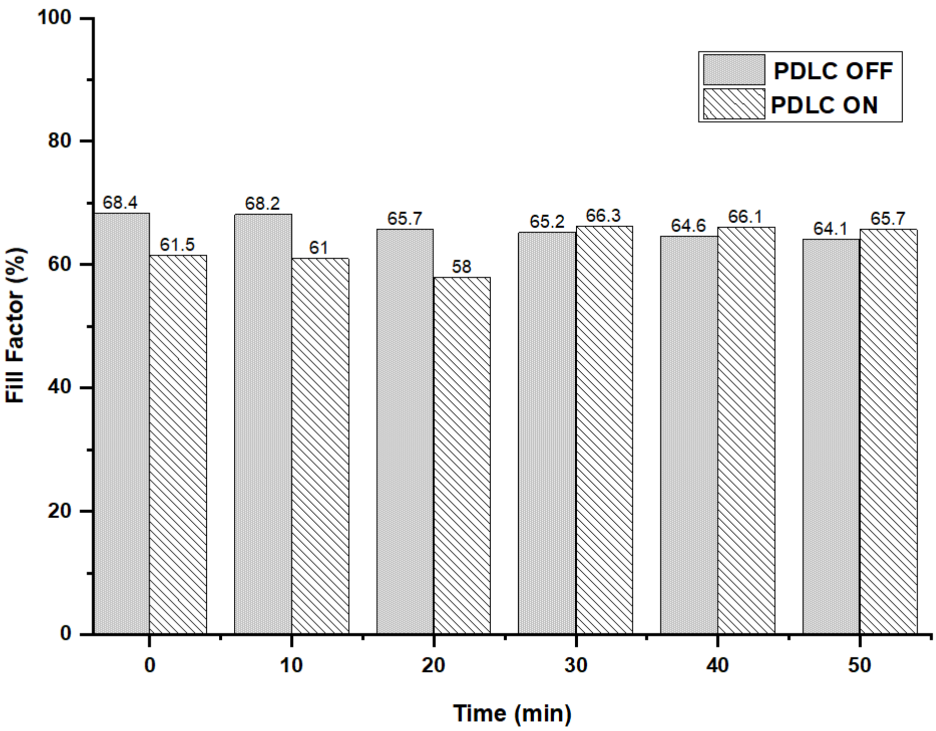

Fig. 12: Variation of the FF with time for the PDLC as an OFF and ON mode.

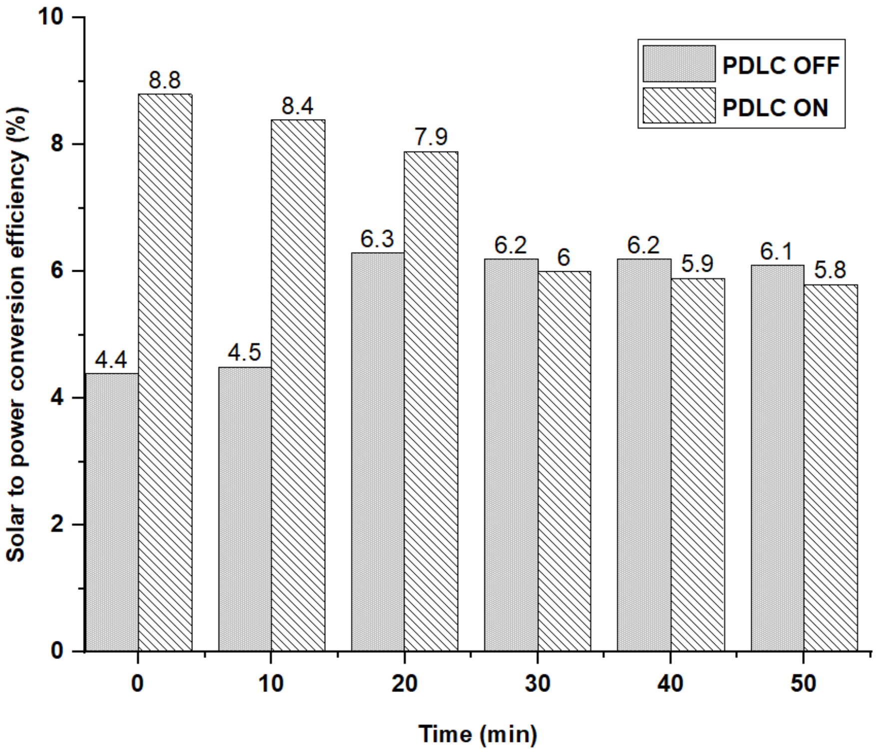

Fig. 13: Variation of the Efficiency of SEH module with time for PDLC as an ON and OFF mode.

4. Conclusion

Here, previously reported low concentrating photovoltaic module was tested to maintain and reduce the operating temperature of the solar cell. The Argon filled LCPV module was tested as well as PDLC films were integrated on top of the LCPV modules while the film was ON and OFF state. It was observed that the operating temperature of the solar cell was reduced by almost 10°C when the LCPV module was filled with Argon. In some cases, although the temperature reduced the efficiency was not improved due to the reduction of the FF, which may be due to the increase of series resistance. Besides, the introduction of the PDLC film on top of the LCPV module showed interesting phenomena for solar to electrical conversion efficiency and the FF of the module. When the PDLC film was OFF mode, it provides larger effect to the FF of the solar cell than that of compared to the PDLC film when it was ON state. Finally, the above work shows a greater potential of using Argon gas filled LCPV module and PDLC film on top of the LCPV modules to regulate its temperatures, however, further experimentation is needed to understand the know-how of such phenomena.

Acknowledgements

This work is funded by JUICE flexible networking funding to Maria Khalid, a project funded by Engineering and Physical Science Research Council (EP/P003605/1).

Reference

[1] P. Yadav, B. Tripathi, S. Rathod, M. Kumar, Real-time analysis of low-concentration photovoltaic systems: A review towards development of sustainable energy technology, Renew. Sustain. Energy Rev. 28 (2013) 812–823. doi:10.1016/j.rser.2013.08.047.

[2] G. Li, Q. Xuan, M.W. Akram, Y. Golizadeh Akhlaghi, H. Liu, S. Shittu, Building integrated solar concentrating systems: A review, Appl. Energy. 260 (2020) 114288. doi:10.1016/j.apenergy.2019.114288.

[3] M. Tian, Y. Su, H. Zheng, G. Pei, G. Li, S. Riffat, A review on the recent research progress in the compound parabolic concentrator (CPC) for solar energy applications, Renew. Sustain. Energy Rev. 82 (2018) 1272–1296. doi:10.1016/j.rser.2017.09.050.

[4] Y. Amanlou, T.T. Hashjin, B. Ghobadian, G. Najafi, R. Mamat, A comprehensive review of Uniform Solar Illumination at Low Concentration Photovoltaic (LCPV) Systems, Renew. Sustain. Energy Rev. 60 (2016) 1430–1441. doi:10.1016/j.rser.2016.03.032.

[5] Y. Sun, K. Shanks, H. Baig, W. Zhang, X. Hao, Y. Li, B. He, R. Wilson, H. Liu, S. Sundaram, J. Zhang, L. Xie, T. Mallic, Y. Wu, Integrated CdTe PV glazing into windows: Energy and daylight performance for different window-to-wall ratio, Energy Procedia. 158 (2019) 3014–3019. doi:10.1016/j.egypro.2019.01.976.

[6] J. Nilsson, M. Brogren, A. Helgesson, A. Roos, B. Karlsson, Biaxial model for the incidence angle dependence of the optical efficiency of photovoltaic systems with asymmetric reflectors, Sol. Energy. 80 (2006) 1199–1212. doi:10.1016/j.solener.2005.09.008.

[7] B. Perers, B. Karlsson, COLLECTOR ARRAYS , SIMULATION MODEL AND EXPERIMENTAL RESULTS, 51 (1993) 327–337.

[8] D. Chemisana, Building integrated concentrating photovoltaics: A review, Renew. Sustain. Energy Rev. 15 (2011) 603–611. doi:10.1016/j.rser.2010.07.017.

[9] N. Sarmah, B.S. Richards, T.K. Mallick, Evaluation and optimization of the optical performance of low-concentrating dielectric compound parabolic concentrator using ray-tracing methods, Appl. Opt. 50 (2011) 3303–3310. doi:10.1364/AO.50.003303.

[10] A. Rabl, J. O'Gallagher, R. Winston, Design and test of non-evacuated solar collectors with

compound parabolic concentrators, Sol. Energy. 25 (1980) 335–351. doi:10.1016/0038-092X(80)90346-1.

[11] A.S. Jadhav, A.S. Gudekar, R.G. Patil, D.M. Kale, S. V. Panse, J.B. Joshi, Performance analysis of a novel and cost effective CPC system, Energy Convers. Manag. 66 (2013) 56–65. doi:10.1016/j.enconman.2012.09.030.

[12] H. Baig, N. Sellami, D. Chemisana, J. Rosell, T.K. Mallick, Performance analysis of a dielectric based 3D building integrated concentrating photovoltaic system, Sol. Energy. 103 (2014) 525–540. doi:10.1016/j.solener.2014.03.002.

[13] X. Li, Y.J. Dai, Y. Li, R.Z. Wang, Performance investigation on a novel single-pass evacuated tube with a symmetrical compound parabolic concentrator, Sol. Energy. 98 (2013) 275–289. doi:10.1016/j.solener.2013.10.015.

[14] W. Li, M.C. Paul, N. Sellami, T. Sweet, A. Montecucco, J. Siviter, H. Baig, M. Gao, T. Mallick, A. Knox, Six-parameter electrical model for photovoltaic cell/module with compound parabolic concentrator, Sol. Energy. 137 (2016) 551–563. doi:10.1016/j.solener.2016.08.050.

[15] M. Al-Shidhani, M. Al-Najideen, V.G. Rocha, G. Min, Design and testing of 3D printed cross compound parabolic concentrators for LCPV system, AIP Conf. Proc. 2012 (2018). doi:10.1063/1.5053489.

[16] T.K. Mallick, P.C. Eames, B. Norton, Power losses in an asymmetric compound parabolic photovoltaic concentrator, Sol. Energy Mater. Sol. Cells. 91 (2007) 1137–1146. doi:10.1016/j.solmat.2007.03.020.

[17] N. Sarmah, T.K. Mallick, Design, fabrication and outdoor performance analysis of a low concentrating photovoltaic system, Sol. Energy. 112 (2015) 361–372. doi:10.1016/j.solener.2014.12.019.

[18] N. Sellami, T.K. Mallick, Optical characterisation and optimisation of a static Window Integrated Concentrating Photovoltaic system, Sol. Energy. 91 (2013) 273–282. doi:10.1016/j.solener.2013.02.012.

[19] P. Zielonka, E. Gierlik, M. Matejak, K. Dolowy, The comparison of experimental and theoretical temperature distribution during microwave wood heating, Holz Als Roh - Und Werkst. 55 (1997) 395–398. doi:10.1007/s001070050253.

[20] J.K. Kaldellis, M. Kapsali, K.A. Kavadias, Temperature and wind speed impact on the efficiency of PV installations. Experience obtained from outdoor measurements in Greece, Renew. Energy. 66 (2014) 612–624. doi:10.1016/j.renene.2013.12.041.

[21] O. Dupré, R. Vaillon, M.A. Green, Physics of the temperature coefficients of solar cells, Sol. Energy Mater. Sol. Cells. 140 (2015) 92–100. doi:10.1016/j.solmat.2015.03.025.

[22] K. Shanks, A. Knowles, A. Brierley, H. Baig, H. Orr, Y. Sun, Y. Wu, S. Sundaram, T. Mallick, An experimental analysis of the optical, thermal and power to weight performance of plastic and glass optics with AR coatings for embedded CPV windows, Sol. Energy Mater. Sol. Cells. 200 (2019) 110027. doi:10.1016/j.solmat.2019.110027.

[23] M.G. Deceglie, T.J. Silverman, B. Marion, S.R. Kurtz, Metastable changes to the temperature coefficients of thin-film photovoltaic modules, 2014 IEEE 40th Photovolt. Spec. Conf. PVSC 2014. 15 (2014) 337–340. doi:10.1109/PVSC.2014.6924926.

[24] S. Dubey, J.N. Sarvaiya, B. Seshadri, Temperature dependent photovoltaic (PV) efficiency and its effect on PV production in the world - A review, Energy Procedia. 33 (2013) 311–321. doi:10.1016/j.egypro.2013.05.072.

[25] E. Skoplaki, J.A. Palyvos, Operating temperature of photovoltaic modules: A survey of

pertinent correlations, Renew. Energy. 34 (2009) 23–29. doi:10.1016/j.renene.2008.04.009.

[26] E. Skoplaki, J.A. Palyvos, On the temperature dependence of photovoltaic module electrical performance: A review of efficiency/power correlations, Sol. Energy. 83 (2009) 614–624. doi:10.1016/j.solener.2008.10.008.

[27] H. Baig, K.C. Heasman, T.K. Mallick, Non-uniform illumination in concentrating solar cells, Renew. Sustain. Energy Rev. 16 (2012) 5890–5909. doi:10.1016/j.rser.2012.06.020.

[28] T. Nehari, M. Benlakam, D. Nehari, Effect of the fins length for the passive cooling of the photovoltaic panels, Period. Polytech. Mech. Eng. 60 (2016) 89–95. doi:10.3311/PPme.8571.

[29] F. Grubišić-Čabo, S. Nižetić, T.G. Marco, Photovoltaic panels: A review of the cooling techniques, Trans. Famena. 40 (2016) 63–74.

[30] A. Hasan, H. Alnoman, A.H. Shah, Energy efficiency enhancement of photovoltaics by phase change materials through thermal energy recovery, Energies. 9 (2016). doi:10.3390/en9100782.

[31] M.J. Huang, P.C. Eames, N.J. Hewitt, The application of a validated numerical model to predict the energy conservation potential of using phase change materials in the fabric of a building, Sol. Energy Mater. Sol. Cells. 90 (2006) 1951–1960. doi:10.1016/j.solmat.2006.02.002.

[32] A. Hasan, S.J. McCormack, M.J. Huang, B. Norton, Energy and cost saving of a photovoltaic-phase change materials (PV-PCM) System through temperature regulation and performance enhancement of photovoltaics, Energies. 7 (2014) 1318–1331. doi:10.3390/en7031318.

[33] S. Sharma, A. Tahir, K.S. Reddy, T.K. Mallick, Performance enhancement of a Building-Integrated Concentrating Photovoltaic system using phase change material, Sol. Energy Mater. Sol. Cells. 149 (2016) 29–39. doi:10.1016/j.solmat.2015.12.035.

[34] L.M. Candanedo, A. Athienitis, K.W. Park, Convective heat transfer coefficients in a building-integrated photovoltaic/thermal system, J. Sol. Energy Eng. Trans. ASME. 133 (2011) 1–14. doi:10.1115/1.4003145.

[35] K. Araki, H. Uozumi, M. Yamaguchi, A simple passive cooling structure and its heat analysis for 500 X concentrator PV module, Conf. Rec. IEEE Photovolt. Spec. Conf. (2002) 1568–1571. doi:10.1109/pvsc.2002.1190913.

[36] W.G. Anderson, P.M. Dussinger, D.B. Sarraf, S. Tamanna, Heat pipe cooling of concentrating photovoltaic cells, Conf. Rec. IEEE Photovolt. Spec. Conf. (2008). doi:10.1109/PVSC.2008.4922577.

[37] M. Abdolzadeh, M. Ameri, Improving the effectiveness of a photovoltaic water pumping system by spraying water over the front of photovoltaic cells, Renew. Energy. 34 (2009) 91–96. doi:10.1016/j.renene.2008.03.024.

[38] N. Lolli, I. Andresen, Aerogel vs. argon insulation in windows: A greenhouse gas emissions analysis, Build. Environ. 101 (2016) 64–76. doi:10.1016/j.buildenv.2016.03.001.

[39] N. Ehrmann, R. Reineke-Koch, S. Föste, F. Giovannetti, The influence of process parameters and coating properties of double glazing coated with transparent conducting oxides on the efficiency of solar-thermal flat-plate collectors, Thin Solid Films. 532 (2013) 132–140. doi:10.1016/j.tsf.2012.11.145.

[40] T. Baenas, M. Machado, On the analytical calculation of the solar heat gain coefficient of a BIPV module, Energy Build. 151 (2017) 146–156. doi:10.1016/j.enbuild.2017.06.039.

[41] A. Ghosh, B. Norton, A. Duffy, Effect of sky clearness index on transmission of evacuated (vacuum) glazing, Renew. Energy. 105 (2017) 160–166. doi:10.1016/j.renene.2016.12.056.

[42] A. Ghosh, N. Sarmah, S. Sundaram, T.K. Mallick, Numerical studies of thermal comfort for semi-transparent building integrated photovoltaic (BIPV) -vacuum glazing system, Sol. Energy. 190 (2019) 608–616. doi:10.1016/j.solener.2019.08.049.

[43] A. Ghosh, S. Sundaram, T.K. Mallick, Investigation of thermal and electrical performances of a combined semi- transparent PV-vacuum glazing, Appl. Energy. 228 (2018) 1591–1600. doi:10.1016/j.apenergy.2018.07.040.

[44] A. Ghosh, B. Norton, Advances in switchable and highly insulating autonomous (self-powered) glazing systems for adaptive low energy buildings, Renew. Energy. 126 (2018) 1003–1031. doi:10.1016/j.renene.2018.04.038.

[45] A. Ghosh, T.K. Mallick, Evaluation of optical properties and protection factors of a PDLC switchable glazing for low energy building integration, Sol. Energy Mater. Sol. Cells. (2017) 0–1. doi:10.1016/j.solmat.2017.10.026.

[46] A. Ghosh, T.K. Mallick, Evaluation of colour properties due to switching behaviour of a PDLC glazing for adaptive building integration, Renew. Energy. 120 (2018) 126–133. doi:10.1016/j.renene.2017.12.094.

[47] A. Ghosh, B. Norton, T.K. Mallick, Influence of atmospheric clearness on PDLC switchable glazing transmission, Energy Build. 172 (2018) 257–264. doi:10.1016/j.enbuild.2018.05.008.

[48] A. Ghosh, B. Norton, T.K. Mallick, Daylight characteristics of a polymer dispersed liquid crystal switchable glazing, Sol. Energy Mater. Sol. Cells. 174 (2018) 572–576. doi:10.1016/j.solmat.2017.09.047.

[49] E. Cuce, Accurate and reliable U-value assessment of argon-filled double glazed windows: A numerical and experimental investigation, Energy Build. 171 (2018) 100–106. doi:10.1016/j.enbuild.2018.04.036.

[50] J. Li, Y. Tian, S. Sun, J. Li, L. Zhang, Advanced Functional Materials, Springer Singapore, 2018. doi:10.1007/978-981-13-0110-0.

[51] P. Singh, N.M. Ravindra, Analysis of series and shunt resistance in silicon solar cells using single and double exponential models, Emerg. Mater. Res. 1 (2012) 33–38. doi:10.1680/emr.11.00008.

[52] A. Ben Or, J. Appelbaum, Dependence of multi-junction solar cells parameters on concentration and temperature, Sol. Energy Mater. Sol. Cells. 130 (2014) 234–240. doi:10.1016/j.solmat.2014.07.010.